View metadata, citation and similar papers at core.ac.uk

brought to you by CORE

provided by UWE Bristol Research Repository

Electrochemistry Communications 75 (2017) 38–42

Contents lists available at ScienceDirect

Electrochemistry Communications

journal homepage: www.elsevier.com/locate/elecom

Transition metal-nitrogen-carbon catalysts for oxygen reduction reaction in neutral electrolyte

Santiago Rojas-Carbonell, Carlo Santoro, Alexey Serov, Plamen Atanassov *

Chemical and Biological Engineering Department, Center for Micro-Engineered Materials (CMEM), University of New Mexico, 1001 University Blvd. SE, Albuquerque, NM, USA

ARTICLE INFO

Article history:
Received 7 November 2016
Received in revised form 15 December 2016
Accepted 16 December 2016
Available online 21 December 2016

Keywords:
ORR
PGM-free
Current production
Electron transfer
Neutral pH

ABSTRACT

Platinum group metal-free (PGM-free) catalysts based on M-N-C types of materials with M as Mn, Fe, Co and Ni and aminoantipyrine (AAPyr) as N-C precursors were synthesized using sacrificial support method. Catalysts kinetics of oxygen reduction reaction (ORR) was studied using rotating ring disk electrode (RRDE) in neutral pH. Results showed that performances were distributed among the catalysts as: Fe-AAPyr > Co-AAPyr > Mn-AAPyr > Ni-AAPyr. Fe-AAPyr had the highest onset potential and half-wave potential. All the materials showed similar limiting current. Fe-AAPyr had an electron transfer involving $4e^-$ with peroxide formed lower than 5%. Considering H_2O_2 produced, it seems that Co-AAPyr, Mn-AAPyr and Ni-AAPyr follow a $2 \times 2e^-$ mechanism with peroxide formed during the intermediate step. Durability test was done on Fe-AAPyr for 10,000 cycles. Decrease of activity was observed only after 10,000 cycles.

© 2016 The Authors. Published by Elsevier B.V. This is an open access article under the CC BY license (http://creativecommons.org/licenses/by/4.0/).

1. Introduction

Oxygen reduction reaction (ORR) at the cathode is often the limiting steps in the reduction reactions happening generally into FCs dealing with fuels like hydrogen [1–2]. Those limitations have been studied deeply in acidic and alkaline environments but not in neutral media [2–5]. ORR follows different patterns in function of the pH environment in which the reaction occurs. H^+ and OH^- are required to complete the reaction in acidic and alkaline media respectively [6–7]. Neutral media (pH = 7) has a low concentration (10^{-7} M) of H^+ and OH^- that affects negatively the ORR kinetics. High overpotentials are shown in the existing literature [2–5].

Microbial fuel cells (MFCs) operate at neutral conditions and room temperature in order to allow bacteria activity and survivor and this lowers the ORR performances. Catalysts are then used to enhance the reaction rate. Three different typologies of catalysts are investigated in MFC [3–5].

The first one is based on platinum group metals as inheritance of the most studied acidic or alkaline fuel cells. This choice cannot be justified due to the high catalyst cost compared to the low power output produced. Moreover, MFCs operates in very polluted environment and interaction of anions with Pt is known to deactivate the catalytic activity in short time [8–10].

The second choice has been introduced in the past years and it concerns the utilization of carbonaceous-based materials but unfortunately overpotentials are very high and kinetics remains weak [11–12].

The third choice is the utilization of M-N-C types of catalysts in which M can be platinum group metal (PGM) [13–16] or completely PGM-free with M being an earth abundant transition metal like Mn, Fe, Co and Ni. M-N-C catalysts were deeply studied in acidic and alkaline media [17–20] and recently the most pursued in neutral media [3–5,21–25]. PGM-free catalysts showed high performances and durability in long terms operations compared to Pt [9–10,26].

Only few mechanistic studies showing catalysts kinetics in neutral media are presented in literature focusing on Fe-based [24,27–29] or carbonaceous catalysts [30–31]. None of the studies faced the mechanistic activity and the kinetics of M-N-C with M as Co, Ni and Mn that are the other earth abundant metals together with Fe mostly used to substitute the more expensive Pt. Kinetics behavior of those catalysts is quite elusive and not well understood. Moreover, H_2O_2 yield production, electron transfer mechanisms and loading effect on kinetic current density have not been shown for any catalysts working in neutral media.

In this work, we studied the kinetics of four PGM-free catalysts based on the same synthetic process and the same precursors (aminoantipyrine) using rotating ring disk electrode (RRDE) method. Disk current, Tafel plots, H_2O_2 production, electron transfer and loading effect on kinetic current density are discussed. Durability test (10,000 cycles) on Fe-AAPyr is presented and a comparison with Pt is shown. This work enhances the understanding of PGM-free catalysts working in neutral conditions.

* Corresponding author at: University of New Mexico, Department of Chemical & Biological Engineering, Center for Micro-Engineered Materials, 87131 Albuquerque, NM, United States.
E-mail address: plamen@unm.edu (P. Atanassov).

http://dx.doi.org/10.1016/j.elecom.2016.12.011
1388-2481/© 2016 The Authors. Published by Elsevier B.V. This is an open access article under the CC BY license (http://creativecommons.org/licenses/by/4.0/).

2. Materials and method

2.1. Catalysts preparation

Sacrificial support method (SSM) was used to synthesis the catalysts investigated. Aminoantipyrine (AAPyr) was used as organic precursor for the synthesis. ($Fe(NO_3)_3 \times 9H_2O$, $Co(NO_3)_2 \times 6H_2O$, $Mn(NO_3)_2 \times 4H_2O$, $Ni(NO_3)_2 \times 6H_2O$) were the metallic salts mixed with AAPyr and impregnated with fumed silica (~250 $m^2\ g^{-1}$). Ball milling was used to ground the mixed materials. Heat treatment was then applied in a constant flow (100 mL min^{-1}) of UHP nitrogen. Temperature was raised till 950 °C (25 °C min^{-1}) and stabilized for 30 min. After pyrolysis, the mixture was cool down at room temperature and silica was etched using 20 wt% HF for 12 h. The catalyst was washed and then dried overnight. Obtained catalysts were named in function of the metal used that was Mn, Fe, Co, Ni.

2.2. Electrochemical measurements and analysis

Rotating ring disk electrode (RRDE) technique on Mn-AAPyr, Fe-AAPyr, Co-AAPyr, Ni-AAPyr inks was used to evaluate the catalysts kinetics. The inks were prepared uniformly suspending 5 mg of each catalyst into 0.075% of 1100 EW Nafion solution (FuelCellStore, USA) and then sonicating for three times (30 s) for a correct dispersion. Different loadings (50, 100, 200, 400 and 600 μg cm^{-2}) were tested. Experiments were done in neutral conditions with electrolyte solution composed by potassium phosphate buffer (0.1 M) and KCl (0.1 M). The solution was purged with pure oxygen for over 30 min. RRDE setup allows to measure the disk current produced by the catalysts and also the peroxide produced as intermediate of the $4e^-$ transfer through the ring current. Linear sweep voltammetry (LSV) was run from 1.08 V to 0.18 V (vs RHE) at scan rate of 5 mV s^{-1} in separate triplicates. Disk (j_D) and ring (j_R) currents densities are correlated by Eq. (1) in which the electrons transferred are estimated.

$$n = \left|\frac{4 \times j_D}{j_D - j_R}\right| \tag{1}$$

The estimated electrons transferred are also used for identifying the H_2O_2 produced (%) during the ORR process as showed by Eq. (2):

$$x = \frac{4-n}{2} \times 100 \tag{2}$$

Durability tests were done to Fe-AAPyr (loading 600 μg cm^{-2}) cycling 10,000 times from 1.08 V to 0.18 V (vs RHE) at scan rate of 50 mV s^{-1}. The acquisition of the reported LSV (10, 100, 1000, 3000 and 10,000 cycles) was done at scan rate of 5 mV s^{-1}.

Koutecky-Levich equation Eq. (3) was used and $|i_d|^{-1}$ was plot against ω^{-1}. i_k and n can be extrapolated from the system.

$$\frac{1}{j_d} = \frac{1}{j_k} + \frac{1}{0.62nFC_{O2}D_{O2}^{2/3}\nu^{-1/6}\omega^{1/2}A} \tag{3}$$

i_k is the electrode potential dependent kinetic current density of the ORR, n is the average number of electrons transferred per catalytic event (4 is the maximum), F is the Faraday's constant (96,487 C mol^{-1}), C_{O2} is the concentration of O_2 in the electrolyte ($1.117e^{-6}$ mol mL^{-1}), D_{O2} is the O_2 diffusion coefficient in aqueous media ($1.9e^{-5}$ $cm^2\ s^{-1}$), and ν is the kinetic viscosity of the electrolyte (0.01073 $cm^2\ s^{-1}$), ω is the angular momentum in rad·s^{-1}, and A is the electrode sectional area.

3. Results and discussion

3.1. Disk current, e^- transfer mechanism and H_2O_2 production

Disk currents (Fig. 1a), electrons transferred (Fig. 1b) and peroxide yields (Fig. 1c) are here presented for every catalyst. Different trends can be noticed into the disk current (Fig. 1a). Higher onset potential was measured by Fe-AAPyr (0.98 V (vs RHE)) followed by Co-AAPyr (0.892 V (vs RHE)), Mn-AAPyr (0.864 V (vs RHE)) and Ni-AAPyr (0.802 V (vs RHE)). The onset potential trends followed the current densities produced from the kinetic limited region until reaching the transport limited plateau. Fe-AAPyr had the highest disk current followed by Co-AAPyr, Mn-AAPyr and Ni-AAPyr with the latter as the lowest value measured (Fig. 1a). Fe-AAPyr, Co-AAPyr and Mn-AAPyr reached a similar diffusion limited current at 0.185 V (vs RHE) quantified as ≈4.5 mA cm^{-2}. Ni-AAPyr had current of ≈4 mA cm^{-2} at that same potential. As for the half-wave potential, the trend is as follows: 0.807 V for Fe, 0.782 V for Co, 0.716 V Mn and 0.571 V for Ni. The electrons transferred at 0.185 V (vs RHE) are estimated to be between 3.5 and 4 with exact number of 3.96 for Fe-AAPyr, 3.84 for Co-AAPyr, 3.67 for Mn-AAPyr and 3.64 for Ni-AAPyr (Fig. 1b). Interestingly, at higher potentials Co-AAPyr and Ni-AAPyr had lower electron transferred of 3.00 and 2.87 respectively (Fig. 1b). Also Mn-AAPyr had slightly lower number of electron transferred (3.50) at higher potential (Fig. 1b). At the contrary, Fe-AAPyr was the only catalysts showing the same electrons transferred (3.96) along the range investigated (Fig. 1b). Peak peroxide yield of 50%, 24% and 56% was formed by Co-AAPyr, Mn-AAPyr and Ni-AAPyr respectively at lower overpotentials investigated (Fig. 1c). Fe-AAPyr had low production of peroxide quantified in 2–3%. Peroxide data are necessary for further explaining the electron transfer mechanisms involving the catalysts investigated. In fact, Fe-AAPyr seems to have an apparent direct $4e^-$ transfer mechanism, evidenced by low peroxide production. This mechanism is preferred since the maximum number of electrons is electrochemically transferred during the reaction. In contrast, the high peroxide produced at low overpotentials for Co-AAPyr, Mn-AAPyr and Ni-AAPyr indicates that the peroxide intermediate is produced and then electrochemically oxidized to water at higher overpotentials. This allows to speculate that probably those catalysts have $2 \times 2e^-$ transfer mechanisms during ORR. Peroxide production in MFCs is an undesired process since peroxide can negatively affect the electroactive bacteria on the anode electrode. Those results indicated a superior electrocatalytic activity of Fe-AAPyr compared to the other PGM-free catalysts investigated. The origin of such selectivity towards a $4e^-$ mechanism for the Fe based catalyst versus the $2 \times 2e^-$ transfer mechanism for the other metals has been modeled by density functional theory calculations [32–34].

3.2. Effect of loading on ORR kinetics

The effect of the catalyst loading on the ORR kinetics was studied for Fe-AAPyr, as it was the best performing catalysts investigated (Fig. 2). Limiting current densities enhanced substantially increasing the loading from 50 to 200 μg cm^{-2} (Fig. 2a). This indicates that the reaction mechanism of Fe-AApyr follows a $2 \times 2e^-$ transfer process, as an increase in loading increases the limiting current densities and decreases the peroxide yield (Fig. 2c). This is due to a fast H_2O_2 reduction within the catalytic layer, conclusion that is supported by the $4e^-$ transfer mechanism seen at all potentials and loadings (Fig. 2b). H_2O_2 peroxide production was always lower than 10% for all the loading investigated. Peroxide decrease with increase of loading is due to H_2O_2 entrapment inside a thicker catalyst layer, being further reduced before reaching the platinum ring (Fig. 2c).

Fig. 2d displays the kinetic current densities calculated by the Koutecky-Levich analysis for each loading. The increase in kinetic current density between the loadings of 50 and 200 μg cm^{-2} demonstrated that higher availability of active sites within the catalytic layer turn into faster oxygen reduction. This supports the idea of a two-steps electron

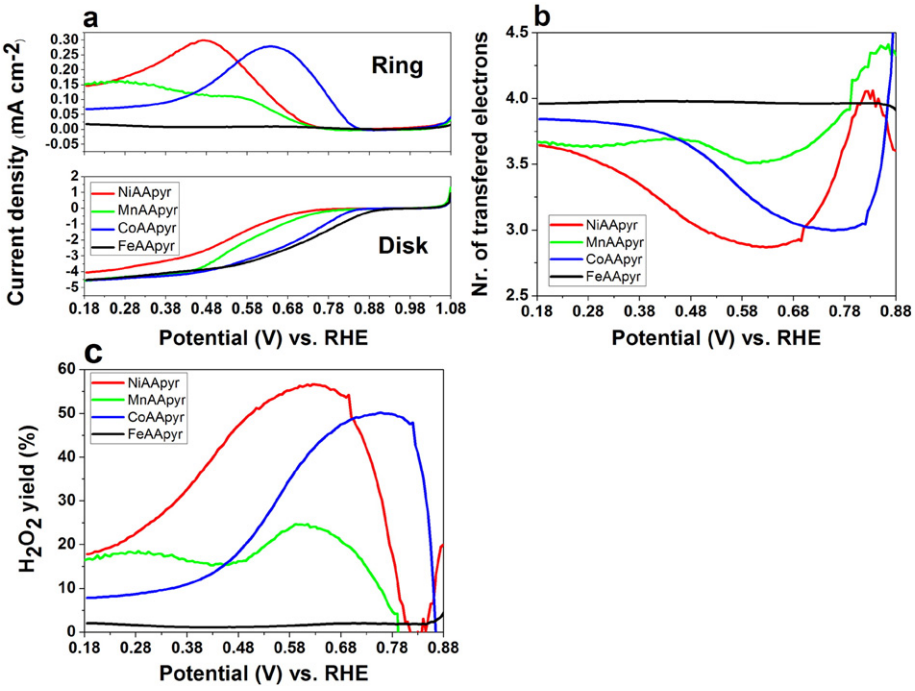

Fig. 1. Disk and ring current densities (a), number of electrons transferred (b) and peroxide yield (c) of Mn-, Fe-, Co- and Ni-AAPyr catalysts (loading 600 μg cm^{-2} and RRDE speed of 1200 rpm).

transfer process, as the peroxide intermediates are more readily reduced to water. A further increase in loading led to a decrease in the kinetic current density, which indicates that probably the reactants are not reaching the active sites fast enough, entrapped inside a thicker catalytic layer. Those results confirm that Fe-AAPyr is an excellent catalyst for ORR in neutral media, yielding high currents and low peroxide evolution.

3.3. Durability tests

Durability test was done on Fe-AAPyr catalyst being the best performing PGM-free catalysts here investigated. Cycles number 10, 100, 1000, 3000 and 10,000 are represented (Fig. 3). Disk current does not change importantly in the first 3000 cycles but only after 10,000 cycles, which is an indicator of the high stability of the catalyst (Fig. 3a). A

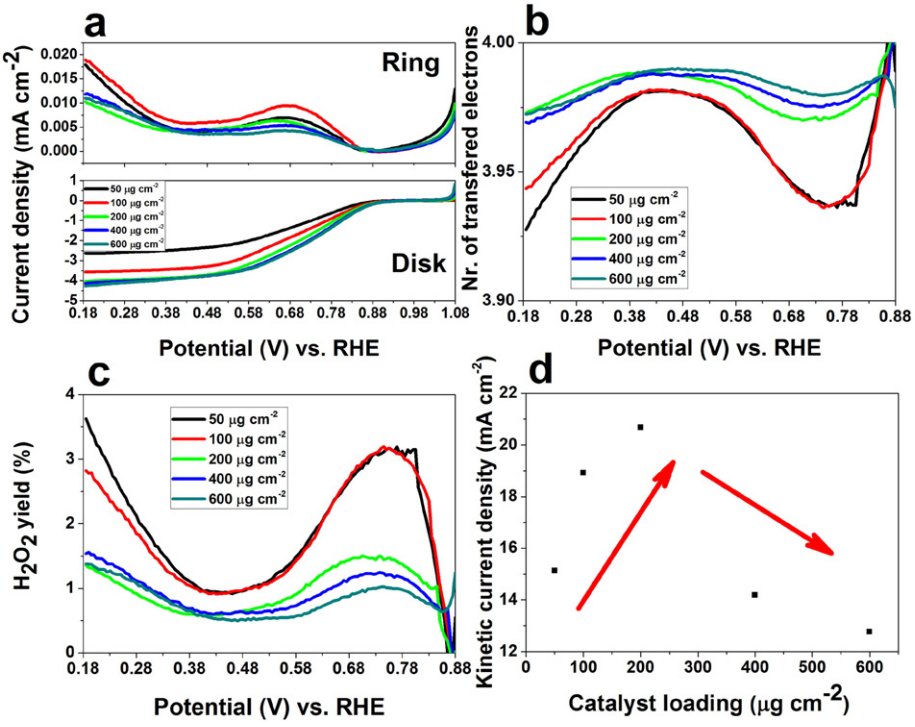

Fig. 2. Disk and ring current densities (a), number of electrons transferred (b) and peroxide yield (c) of Fe-AAPyr catalysts with different loadings, scan rate of 5 mV s^{-1} at 1200 rpm. (d) Kinetic current densities calculated with the Koutecky-Levich analysis at different rotation speeds for five loadings.

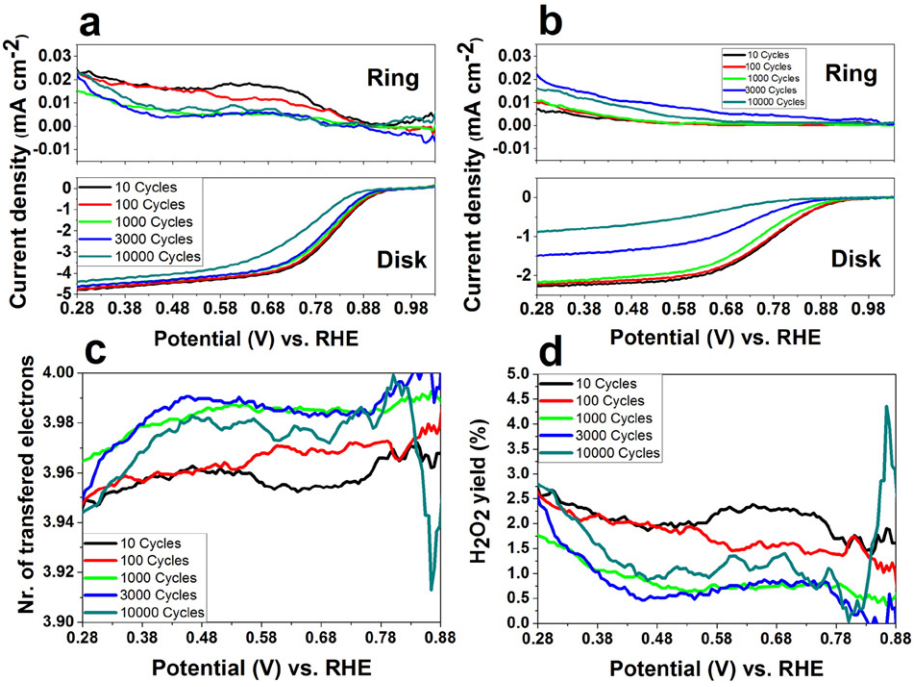

Fig. 3. (a) Disk and ring current densities for Fe-AApyr catalyst after different cycles (loading 600 μg cm^{-2}), (b) Disk and ring current densities for Pt (nominal loading of 0.04 mg cm^{-2}) after different cycles, (c) number of electrons transferred and (d) peroxide yield for Fe-AApyr catalyst after different cycles. Scan rate of 5 mV s^{-1} at 1200 rpm.

reduction of only 2.5% in limiting current was detected between cycle 100 and 3000 and an additional 5% till cycle 10,000 (Fig. 3a). For the case of platinum (Fig. 3b), there was a decrease of 30% in the limiting current density between the cycle 1000 and 3000 and then an additional 40% decrease between the cycle 3000 and 10,000. This indicates the superior stability of Fe-AAPyr over Pt.

Half-wave potential decreased 30% at the 10,000 cycle compared to the beginning of life. This could point towards the degradation of the active sites that carry out the first step of the reaction, the reduction of oxygen to peroxide.

The overall number of electron transferred during the reaction was ≈3.8 after 10,000 cycles (Fig. 3c). In contrast, the peroxide production decreased as the durability test progressed (Fig. 3d), dropping from a yield of 9% (10 cycles) to 5% (10,000 cycles). The decrease is most significant between 100 cycles and 1000 cycles. This phenomenon can be explained by the leaching of peroxide forming species from the Fe-AAPyr catalyst during the cycles. Fe-AAPyr showed high durability in neutral media with a 30% decrease of the half-wave potential after 10,000 cycles and relatively stable in H_2O_2 produced.

4. Conclusions

The effect of the metal towards the ORR catalytic activity was investigated. Fe-AAPyr, Co-AAPyr, Mn-AAPyr and Ni-AAPyr kinetics were compared using the RRDE technique. Results showed that Fe-AAPyr had higher current densities obtained compared to the other catalysts. Fe-AAPyr followed an apparent $4e^-$ transfer mechanism, with low H_2O_2 produced. Electrochemical performances of Co-AAPyr, Mn-AAPyr and Ni-AAPyr showed lower output and electron transfer mechanism that can be speculated as $2 \times 2e^-$ mechanism, in which the second step is not as fast as in the iron containing catalyst. Fe-AAPyr was cycled 10,000 times and stability parameters were studied. Current density decreased 7.5% between the beginning and the end of the 10,000 cycles test. Fe-AAPyr can be considered a valuable catalyst for ORR in neutral media due to its high performances, low H_2O_2 yield and high stability in long terms operations. Superior stability of the PGM-free catalyst was demonstrated when compared with Pt.

Acknowledgement

This work was supported by the Bill & Melinda Gates Foundation (OPP1139954).

References

[1] C. Song, J. Zhang, J. Zhang, Electrocatalytic oxygen reduction reaction, PEM Fuel Cell Electrocatalysts and Catalyst Layers, Springer, Berlin, Germany 2008, pp. 89–134.
[2] M. Shao, Q. Chang, J.-P. Dodelet, R. Chenitz, Recent advances in electrocatalysts for oxygen reduction reaction, Chem. Rev. 116 (2010) 3594–3657.
[3] E. Antolini, Composite materials for polymer electrolyte membrane microbial fuel cells, Biosens. Bioelectron. 69 (2015) 54–70.
[4] Z. Wang, C. Cao, Y. Zheng, S. Chen, F. Zhao, Abiotic oxygen reduction reaction catalysts used in microbial fuel cells, ChemElectroChem 1 (2014) 1813–1821.
[5] H. Yuan, Y. Hou, I.M. Abu Reesh, J. Chen, Z. He, Oxygen reduction reaction catalysts used in microbial fuel cells for energy-efficient wastewater treatment: a review, Mater. Horiz. 3 (2016) 382–401.
[6] K. Kinoshita, Electrochemical Oxygen Technology, John Wiley & Sons, Hoboken NJ, 1992.
[7] B. Erable, D. Feron, A. Bergel, Microbial catalysis of the oxygen reduction reaction for microbial fuel cells: a review, ChemSusChem 5 (2012) 975–987.
[8] K.M. Minachev, N.I. Shuikin, I.D. Rozhdestivenskaya, Poisoning of platinum catalysts with a low content of active metal on a carrier, under conditions of dehydrogenation catalysis, Bull. Acad. Sci. USSR, Div. Chem. Sci. 1 (1952) 567–575.
[9] C. Santoro, A. Serov, C.W. Narvaez Villarrubia, S. Stariha, S. Babanova, K. Artyushkova, A.J. Schuler, P. Atanassov, High catalytic activity and pollutants resistivity using Fe-AAPyr cathode catalyst for microbial fuel cell application, Sci. Rep. 5 (2015) 16596.
[10] C. Santoro, A. Serov, L. Stariha, M. Kodali, J. Gordon, S. Babanova, O. Bretschger, K. Artyushkova, P. Atanassov, Iron based catalysts from novel low-cost organic precursors for enhanced oxygen reduction reaction in neutral media microbial fuel cells, Energy Environ. Sci. 9 (2016) 2346.
[11] F. Zhang, S. Cheng, D. Pant, G. Van Bogaert, B.E. Logan, Power generation using an activated carbon and metal mesh cathode in a microbial fuel cell, Electrochem. Commun. 11 (2009) 2177–2179.
[12] I. Gajda, J. Greenman, C. Melhuish, I. Ieropoulos, Simultaneous electricity generation and microbially-assisted electrosynthesis in ceramic MFCs, Biochemistry 104 (2015) 58–64.
[13] S. Diodati, E. Negro, K. Vezzù, V. Di Noto, S. Gross, Oxygen reduction reaction and X-ray photoelectron spectroscopy characterisation of carbon nitride-supported bimetallic electrocatalysts, Electrochim. Acta 215 (2016) 398–409.
[14] V. Di Noto, E. Negro, K. Vezzù, F. Bertasi, G. Nawn, Origins, developments, and perspectives of carbon nitride-based electrocatalysts for application in low-temperature FCs, Electrochem. Soc. Interface Summer 24 (2) (2015) 59–64.
[15] E. Negro, K. Vezzù, F. Bertasi, P. Schiavuta, L. Toniolo, S. Polizzi, V. Di Noto, Interplay between nitrogen concentration, structure, morphology, and electrochemical

performance of PdCoNi "Core–Shell" carbon nitride electrocatalysts for the oxygen reduction reaction, ChemElectroChem 1 (2014) 1359–1369.
[16] V. Di Noto, E. Negro, S. Polizzi, K. Vezzù, L. Toniolo, G. Cavinato, Synthesis, studies and fuel cell performance of "core–shell" electrocatalysts for oxygen reduction reaction based on a $PtNi_x$ carbon nitride "shell" and a pyrolyzed polyketone nanoball "core", Int. J. Hydrog. Energy 39 (2014) 2812–2827.
[17] A. Serov, M.H. Robson, B. Halevi, K. Artyushkova, P. Atanassov, Highly active and durable templated non-PGM cathode catalysts derived from iron and aminoantipyrine, Electrochem. Commun. 22 (2012) 53–56.
[18] A. Serov, K. Artyushkova, N.I. Andersen, S. Stariha, P. Atanassov, Original mechanochemical synthesis of non-platinum group metals oxygen reduction reaction catalysts assisted by sacrificial support method, Electrochim. Acta 179 (2015) 154–160.
[19] K. Artyushkova, A. Serov, S. Rojas-Carbonell, P. Atanassov, Chemistry of multitudinous active sites for oxygen reduction reaction in transition metal–nitrogen–carbon electrocatalysts, J. Phys. Chem. C 119 (2015) 25917–25928.
[20] A. Brouzgou, S. Song, Z.-X. Liang, P. Tsiakaras, Non-precious electrocatalysts for oxygen reduction reaction in alkaline media: latest achievements on novel carbon materials, Catalysts 6 (2016) 159.
[21] M.-T. Nguyen, B. Mecheri, A. Iannaci, A. D'Epifanio, S. Licoccia, Iron/polyindole-based electrocatalysts to enhance oxygen reduction in microbial fuel cells, Electrochim. Acta 190 (2016) 388–395.
[22] L. Birry, P. Mehta, F. Jaouen, J.P. Dodelet, S.R. Guiot, B. Tartakovsky, Application of iron-based cathode catalysts in a microbial fuel cell, Electrochim. Acta 56 (2011) 1505–1511.
[23] E. Martin, B. Tartakovsky, O. Savadogo, Cathode materials evaluation in microbial fuel cells: a comparison of carbon, Mn_2O_3, Fe_2O_3 and platinum materials, Electrochim. Acta 58 (2011) 58–66.
[24] M.-T. Nguyen, B. Mecheri, A. D'Epifanio, T.P. Sciarria, F. Adani, S. Licoccia, Iron chelates as low-cost and effective electrocatalyst for oxygen reduction reaction in microbial fuel cells, Int. J. Hydrog. Energy 39 (2014) 6462–6469.
[25] F. Zhao, F. Harnisch, U. Schröder, F. Scholz, P. Bogdanoff, I. Herrmann, Application of pyrolysed iron(II) phthalocyanine and CoTMPP based oxygen reduction catalysts as cathode materials in microbial fuel cells, Electrochem. Commun. 7 (2005) 1405.
[26] X. Zhang, D. Pant, F. Zhang, J. Liu, W. He, B.E. Logan, Long-term performance of chemically and physically modified activated carbons in air cathodes of microbial fuel cells, ChemElectroChem 1 (2014) 1859–1866.
[27] G. Lu, Y. Zhu, L. Lu, K. Xu, H. Wang, Y. Jin, Z.J. Ren, Z. Liu, W. Zhang, Iron-rich nanoparticle encapsulated, nitrogen doped porous carbon materials as efficient cathode electrocatalyst for microbial fuel cells, J. Power Sources 315 (2016) 302–307.
[28] W. Yang, B.E. Logan, Immobilization of a metal–nitrogen–carbon catalyst on activated carbon with enhanced cathode performance in microbial fuel cells, ChemSusChem 9 (16) (2016) 2226–2232.
[29] C. Santoro, A. Serov, S. Rojas Carbonell, L. Stariha, J. Gordon, K. Artyushkova, P. Atanassov, A family of Fe-N-C oxygen reduction electrocatalysts for microbial fuel cell (MFC) application: relationships between surface chemistry and performances, Appl. Catal., B. 205 (2017) 24, http://dx.doi.org/10.1016/j.apcatb.2016.12.013.
[30] V.J. Watson, C.N. Delgado, B.E. Logan, Influence of chemical and physical properties of activated carbon powders on oxygen reduction and microbial fuel cell performance, Environ. Sci. Technol. 47 (2013) 6704.
[31] I. Merino-Jimenez, C. Santoro, S. Rojas-Carbonell, J. Greenman, I. Ieropoulos, P. Atanassov, Carbon-based air-breathing cathodes for microbial fuel cells, Catalysts 6 (2016) 127.
[32] S. Katte, P. Atanassov, B. Kiefer, A density functional theory study of oxygen reduction reaction on non-PGM Fe–N_x–C electrocatalysts, Phys. Chem. Chem. Phys. 16 (2014) 13800.
[33] S. Katte, P. Atanassov, B. Kiefer, Density functional theory study of Ni–N_x/C electrocatalyst for oxygen reduction in alkaline and acidic media, J. Phys. Chem. C 116 (2012) 17378.
[34] S. Katte, P. Atanassov, B. Kiefer, Catalytic activity of Co–N_x/C electrocatalysts for oxygen reduction reaction: a density functional theory study, Phys. Chem. Chem. Phys. 15 (2013) 148.